J Appl Electrochem (2010) 40:463–474
DOI 10.1007/s10800-009-0017-x

ORIGINAL PAPER

Influence of CTAB on the electrochemical behavior of dopamine and on its analytic determination in the presence of ascorbic acid

Silvia Corona-Avendaño · María Teresa Ramírez-Silva · Manuel Palomar-Pardavé · Leonardo Hernández-Martínez · Mario Romero-Romo · Georgina Alarcón-Ángeles

Received: 27 March 2009 / Accepted: 25 September 2009 / Published online: 17 October 2009

Abstract This research work concerns the electrochemical study of dopamine and ascorbic acid in the presence of the cationic surfactant cetyltrimethylammonium bromide. From this study is possible to note that the cetyltrimethylammonium bromide greatest influence was on the dopamine, because it disfavors both its oxidation and reduction, thereby giving a smaller heterogeneous rate constant, k^0, value than in its absence, provoking that the process tends to irreversibility. On the contrary, for the ascorbic acid case, its oxidation was favored; these effects can influence the separation of the dopamine and ascorbic acid voltammetric signals up to 453 mV. Further, the method could be optimized through differential pulse voltammetry to proceed with the analytic determination of dopamine in the presence of ascorbic acid displaying usable analytic parameters, namely: a linearity range of 0–130 μM, a sensitivity of (6.318 ± 0.002) μA mM^{-1}, a detection limit of (11 ± 0.1) μM, and a quantification limit of (37 ± 0.2) μM, which made it possible to effect the quantification on a commercial pharmaceutical sample.

Keywords Dopamine · Ascorbic acid · CTAB · CPE

S. Corona-Avendaño · M. Palomar-Pardavé (✉) · L. Hernández-Martínez · M. Romero-Romo · G. Alarcón-Ángeles
Departamento de Materiales, Universidad Autónoma Metropolitana Azcapotzalco, Av. San Pablo #180, Col. Reynosa-Tamaulipas, C.P. 02200 Mexico, D.F., Mexico
e-mail: mepp@correo.azc.uam.mx

M. T. Ramírez-Silva (✉) · G. Alarcón-Ángeles
Departamento de Química, Universidad Autónoma Metropolitana Iztapalapa, Av. San Rafael Atlixco #186, Col. Vicentina, C.P. 09340 Mexico, D.F., Mexico
e-mail: mtrs218@xanum.uam.mx

1 Introduction

Dopamine (DA) has been identified as one of the most relevant neurotransmitters of the central nervous system, the determination of which has increasingly attracted attention during the last decade, mainly due to its relation with neurodegenerative diseases such as Parkinson's and Alzheimer. On the other hand, considerable investments have been made into the development of pharmaceuticals that involve this species, as it is effectively used for several treatments such as hypertension and other heart diseases [1, 2]. The electrochemical methods [3] have advantages over others, because of the possibility to use a sensitive, tailor-made minielectrode, for the purpose of sensing the neurotransmitters in living organisms [4], for instance. Electrochemical analysis is reliably performed on unmodified electrodes however, some limitations may occur; for example on a bare glassy carbon electrode overlapping oxidation potentials of ascorbic acid (AA) and the catecholamine takes place. Hence, a pronounced interference effect appears that induces poor selectivity and reproducibility [5, 6]. Therefore, several studies have been performed using glassy carbon electrodes [7, 8] modified with several compounds, such as the carbon nanotubes [7–14], which usually tend to elevate developmental costs. Thus, in order to diminish the latter, it has been found that the use of surfactants may be sufficiently justified, given that the molecules bear both, a non-polar region and a charged polar group. Further, the molecules can be strongly adsorbed at solid/solution interfaces such as electrodes [15]. The micellar effect on the electrochemical response of several compounds has turned out to be quite interesting, because the molecules seem to facilitate the adsorption and solubilization of various different electrochemically active compounds in the micellar aggregates; this has been

associated to assorted, mostly interesting and relevant changes, like in the redox potential of the analytes present, in the charge transfer and diffusion coefficients of electrode processes, as well as changes in the stability of electrogenerated intermediates and electrochemical products [16–23]. For example, Rusling [16] has successfully used micelles and other surfactant microstructures to catalyze the electrochemical dehalogenation of organic halides. Kaifer and colleagues [17, 18] reported significant changes in the redox potential and peak current of methylviologen in sodium dodecyl sulfate, SDS, micellar solution. Davidovic et al., [19] found that the rate of electrochemical reduction of *p*-nitrosodiphenylamine decreased in the presence of cetyltrimethylammonium bromide, CTAB, micellar solution while [15] Wen et al., [20, 21] have found recently that the oxidation potential, the electron transfer rate constant and diffusion coefficient of ascorbic acid and its lipophilic derivatives are significantly influenced by CTAB and SDS micelles. Surfactants have also been employed to improve selectivity and sensitivity of electrochemical analysis [16, 22, 23]. Particularly, SDS has been successfully used to separate the DA's and AA's signals [24–26] at pH 7. Moreover, Corona-Avendaño et al., [27] showed that the influence of SDS on the electrochemical behavior of DA in an aqueous solution containing different concentrations of SDS, was to increase the charge transfer reaction rate of the electrochemical oxidation of dopamine when SDS was present in the same solution and that when [SDS] > CMC, dopamine's oxidation becomes an adsorption-controlled process [27]. Subsequently, Alarcón-Ángeles et al., [28] with this information demonstrated the usefulness of SDS micellar aggregates, as selective masking agents, to perform the quantitative determination of DA in the presence of AA using differential pulse voltammetry (DPV) and a carbon paste electrode. The authors showed that this novel methodology displays similar analytical features as those of the electrodes previously proposed in the literature, to perform cost-effective DA quantification [28]. Therefore, in lieu of the aforementioned background, the present research work aims at studying the influence of CTAB on the voltammetry response of DA over a carbon paste electrode (CPE) to conduct the determination of this catecholamine in pharmaceutical samples in the presence of AA.

2 Experimental

2.1 Reagents and chemicals

All solutions were made from Merck's analytical grade reagents and deionized water type 1, 18.2 MΩ resistivity, free from organic matter, obtained from a US Filter PURE-LAB Plus UV. The pH was adjusted with HCl (36%) also from Merck. The solutions were degassed with nitrogen and freshly prepared prior to each determination. They were also protected from the incidence of light during performance of the experiments.

2.2 Instrumentation

The electrochemical determinations were carried out with an Autolab PGSTAT 30 potentiostat–galvanostat. A typical three electrode cell was used where a CPE was the working electrode. The CPE was prepared as usual; mixing the Johnson Matthey 1 μm, 99.9% graphite with nujol; for more details please see Ramírez-Silva et al. [29, 30]. A platinum wire (BAS MW-1032) was the counter electrode, while a saturated Ag/AgCl (BAS MF-2052) was the reference electrode, to which all potentials (E) measured in this work should be referred. The pH readings were done with a TACUSSEL potentiometer LPH 430T pH-METER coupled to a CORNING combined glass electrode, 0–14 pH range.

3 Results and discussion

3.1 Electrochemical characterization of the CTAB

Figure 1A shows the CTAB electrochemical behavior for the system CPE/0.1 M NaCl, x mM CTAB where $x \varepsilon \{0, 0.06, 0.12, 0.14, 0.2, 0.24, 0.3, 0.38, 0.48$ mM$\}$ at pH = 3: the CV without CTAB does not show neither an oxidation nor a reduction peak within the potential range studied. When the CTAB was added to the system, starting from a [CTAB] > 0.06 mM, a reduction peak was recorded, P^1_{red} at 810 mV, which increased its intensity as the surfactant's concentration did so. The shape of the peak suggests that an adsorption process is likely to be taking place. A second reduction peak was recorded, P^2_{red}, initially at −621 mV, however, as the surfactant's concentration increased, it shifted toward smaller potentials and slightly increased its intensity. Also, an oxidation current intensity increase was observed from 800 mV, even at 1,108 mV an oxidation peak started to form, termed P^1_{ox}.

Given that the most representative peak of the voltammetry behavior of CTAB is P^1_{red}, then, in the interest of observing significant changes, a plot of the current, I_p, at 810 mV, as a function of log [CTAB] in M, is shown in Fig. 1B, where it is possible to note two slope changes, one at log [CTAB] = −1.47 that corresponds to a concentration of 0.034 mM, while the second is located at −0.74, that corresponds to a 0.18 mM concentration. These changes correspond to the hemimicellar and critical micellar concentrations, respectively [15, 31].

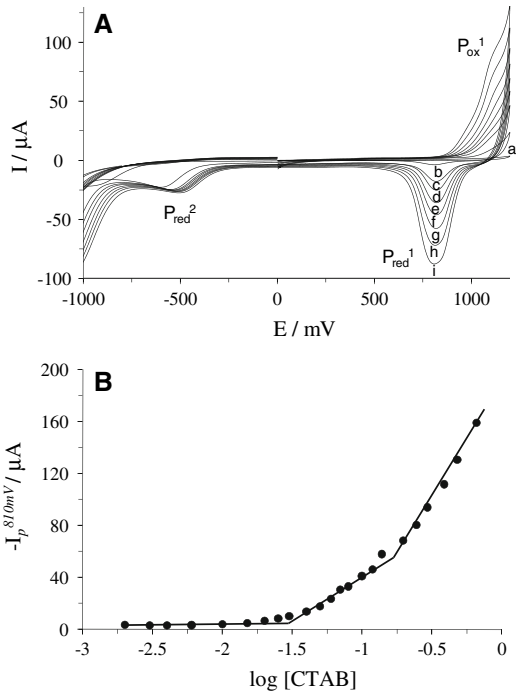

Fig. 1 **A** Family of experimental cyclic voltammograms recorded in the system CPE/x mM CTAB where x is (a) 0, (b) 0.06, (c) 0.12, (d) 0.14, (e) 0.2, (f) 0.24, (g) 0.3, (h) 0.38, and (i) 0.48 mM at pH = 3. **B** Trend of $-I_p$ (810 mV) as a function of log [CTAB]. Potential scan rate 100 mV s^{-1}

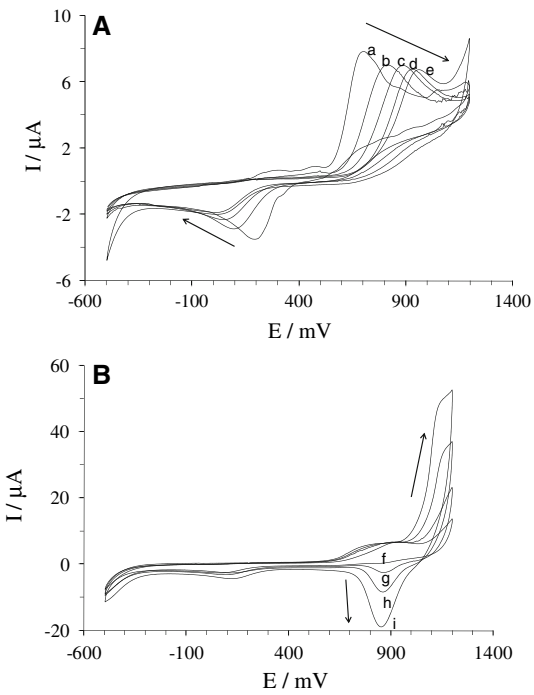

Fig. 2 Family of experimental cyclic voltammograms recorded in the system CPE/DA 0.01 mM, x mM CTAB, where x is (a) 0, (b) 0.004, (c) 0.02, (d) 0.04, (e) 0.2, (f) 0.3, (g) 0.6, (h) 1.3, and (i) 2 mM at pH = 3 and a scan rate of 100 mV s^{-1} for two different [CTAB] concentration ranges **A** $0 \leq x \leq 0.2$ mM and **B** $0.3 \leq x \leq 2$ mM

3.2 Cyclic voltammetry of the DA in the presence of CTAB

Figure 2 shows the CV recorded from the system CPE/0.01 mM DA and x mM CTAB where $x \in \{0, 0.004, 0.02, 0.04, 0.2, 0.3, 0.6, 1.3, 2$ mM$\}$ at pH = 3. Figure 2A depicts that in the absence of CTAB the DA presents an oxidation peak, P_{ox}^{DA}, at 688 mV and a reduction one, P_{red}^{DA}, at 198 mV; the peak separation, ΔE, indicates that the process is not reversible. Corona-Avendaño et al., [27] studied the redox mechanism for the DA on a bare CPE at pH 3, and found that it corresponds to a quasi-reversible process coupled with a chemical reaction [27]. Because both peaks showed a shift in the presence of the CTAB, namely the P_{ox}^{DA} shifted toward larger potentials while the P_{red}^{DA} did so toward smaller potentials, this indicates that the process is becoming more irreversible, until when the [CTAB] was greater than 0.3 mM, refer to Fig. 2B, the P_{ox}^{DA} overlaps with the CTAB signal, though on the other hand, from that concentration a CTAB reduction peak was recorded, thus provoking the P_{red}^{DA} to become imperceptible. This indicates that the cationic properties of the surfactant induce the DA's oxidation and reduction disfavor, due to the presence of the CTAB; this is an outcome that would appear to be the reverse with what happens with the anionic surfactant SDS [27].

Figure 3 shows the trends of the peak currents, I_p, Fig. 3a, and the peak potential, E_p, Fig. 3b, for both: the anodic and cathodic peaks, obtained from the CV of the system described in Fig. 2. It is worthwhile to underline that because the CTAB signal overlaps that of the DA's oxidation peak when the [CTAB] was greater than 0.3 mM, only the trends under such value were analyzed, where a slope change can be noted at 0.034 mM for both cases, which corresponds to the CTAB hemimicellar concentration. However, for values greater than that a change was noted again, although it is not shown, at 0.1 mM that corresponds to the surfactant's CMC.

When an analysis was made of the influence of the CTAB on the DA's electrochemical response, considering the hemimicellar and micellar CTAB concentrations, Fig. 4A shows the CV's recorded for the system CPE/0.01 mM DA, 0.001 mM CTAB at pH = 3, at different potential scan rates, where the [CTAB] is smaller than the hemimicellar value. At 20 mV s^{-1} scan rate, an oxidation peak was recorded at 890 mV, while the reduction peak appeared at 54 mV, which gives a $\Delta E = 836$ mV, with it becoming larger as the rate increased, as can be checked in Table 1.

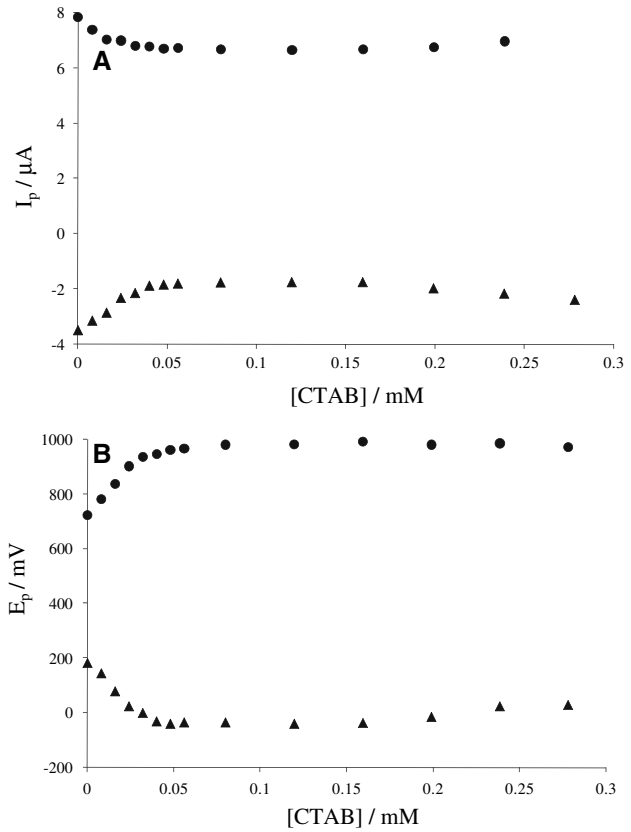

Fig. 3 Trends of the **a** I_p and the **b** E_p measured in the system CPE/DA 0.01 mM, *x* mM CTAB as a function of the [CTAB] for both: the anodic (*filled circle*) and the cathodic (*filled triangle*) peaks

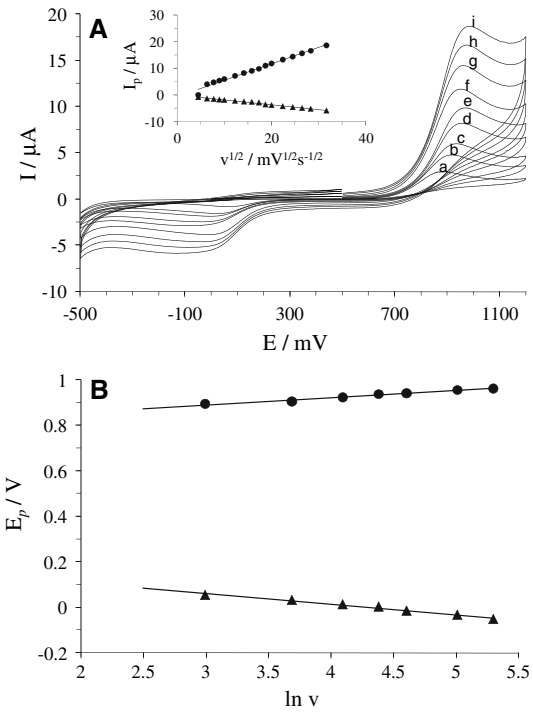

Fig. 4 **A** Experimental CVs recorded in the system CPE/0.1 mM DA, 0.1 M NaCl, 0.001 mM CTAB, at pH = 3.0, with different potential scan rates: (a) 20, (b) 60, (c) 100, (d) 200, (e) 300, (f) 400, (g) 600, (h) 800, and (i) 1,000 mV s^{-1}. The inset shows the variation of I_p, as a function of $v^{1/2}$. The points correspond to the experimental data, while the line is the result of the fitting. **B** Relationship between the peak potential E_p, anodic (*filled circle*) and cathodic (*filled triangle*), and the scan rate, ln *v*, obtained from CVs in Fig. 4a. Lines are the result of the linear fitting procedure

The analysis of the anodic and cathodic I_p as a function of $v^{1/2}$, see inset in Fig. 4A, showed that linearity can be observed for both cases, which suggests that the process is controlled by diffusion. The equations that can be fitted to the linear analysis are, for the anodic case I_p^a (μA) = 0.58 (μA $mV^{-0.5}$ $s^{0.5}$) $v^{1/2}$ + 0.18 (μA) and for the cathodic I_p^c (μA) = −0.18 (μA $mV^{-0.5}$ $s^{0.5}$) $v^{1/2}$ + 0.02 (μA), both with a correlation coefficient of 0.99.

From Table 1, it can be observed that the values obtained for the $|I_{pc}/I_{pa}|$ were smaller than 1, which indicates that CTAB exhibits coupling with a chemical reaction in the DA's redox mechanism, which can also be observed for the DA mechanism without CTAB [25].

Corona-Avendaño et al., [27] evaluated the heterogeneous rate constant, k^0, and the number of electrons transferred for the DA with a CPE in the absence of CTAB, and reported a value of 0.0034 cm s^{-1} and one, respectively.

In order to estimate both k^0, and the number of electrons transferred during DA electrochemical reaction in the presence of CTAB, the variation of the peaks potential as a function of the scan rate was analyzed, see Fig. 4B. Both the anodic and cathodic peak potentials depend linearly on the logarithm of the scan rate as predicted by Eqs. 1 and 3 [27].

Table 1 Variation of the voltammetric parameters as a function of the potential scan rate (*v*) corresponding to the CVs shown in Fig. 4

v (mV s^{-1})	E_{pa} (mV)	E_{pc} (mV)	$E_{pa} - E_{pc}$ (mV)	I_{pa} (μA)	I_{pc} (μA)	$\lvert I_{pc}/I_{pa}\rvert$
40	905	32	873	3.99	−1.3	0.33
80	938	3	935	5.42	−1.7	0.31
100	942	−15	957	5.97	−1.85	0.31
200	963	−30	1015	8.23	−2.45	0.30
500	960	−30	990	13.29	−4.22	0.32
700	970	−39	1009	15.66	−4.88	0.31
1000	990	−120	1110	18.67	−5.84	0.31

$$E_{pa} = E^0 + m\left[0.78 + \ln\left(\frac{D^{1/2}}{k^0}\right) - 0.5\ln m\right] + 0.5m\ln v \quad (1)$$

$$m = \frac{RT}{[(1-\alpha)nF]} \quad (2)$$

$$E_{pc} = E^0 - m'\left[0.78 + \ln\left(\frac{D^{1/2}}{k^0}\right) - 0.5\ln m'\right] - 0.5m'\ln v \quad (3)$$

$$m' = \frac{RT}{[\alpha nF]} \quad (4)$$

where E^0 is the formal potential of DA ($(E_{pa} + E_{pc})/2) = 0.46$ V, D is the diffusion coefficient, k^0 is the heterogeneous standard rate constant, α is the energy transfer coefficient, and n is the number of electrons transferred during the heterogeneous reaction. R, T, and F are the universal gas constant, absolute temperature and Faraday constant, respectively. From the slope and intercept of the straight lines in Fig. 4B and using the reported value of DA's diffusion coefficient, 4.15×10^{-6} cm^2 s^{-1} [27], an average value of k^0 was calculated as 0.00015 cm s^{-1} which when compared to that obtained without CTAB, is much smaller. Therefore, the DA charge transfer in the presence of CTAB is slower, thus disfavoring the oxidation process. From the experimental variation of the anodic peak current (I_{pa}) as a function of $E - E^0$, see Fig. 5, and Eq. 5 [27], it is possible to estimate the value of the energy transfer coefficient, α, which in our case was 0.47. Using this α value, Eqs. 2 and 4 and the slope of lines in Fig. 4B, one can estimate the number of electrons involved during DA oxidation and reduction process 0.95. From this result it is possible to conclude that DA oxidation occurs in this case through monoelectronic steps.

$$I_p = 0.227FAC_0^*k^0\exp\left[-\alpha f\left(E_p - E^0\right)\right] \quad (5)$$

where A is the electrode surface area, C_0^* is the DA concentration and $f = F/RT$.

When performing the same study for other CTAB concentrations below and above the hemimicellar concentration, 0.01 and 0.034, it is possible to conclude that when [CTAB] increased, k^0 decreased, implying thus that the reaction rate is slower and that the processes were diffusion controlled. Further, the value calculated for k^0 at 0.034 mM indicates that the process was irreversible.

The number of electrons transferred can be calculated from the linear fit shown in Fig. 5; note that the process involves 1 electron. Given that the CTAB is positively charged and that at pH = 3 the DA is also positively charged, this should entail an electrostatic interaction that results in a repulsion effect between the CTAB and the DA, which is reflected by the peak shifting, that disfavors oxidation and reduction, consequently the k^0 decreases. This effect is contrary to that obtained with SDS [27], which is negatively charged, thus inducing the DA's adsorption.

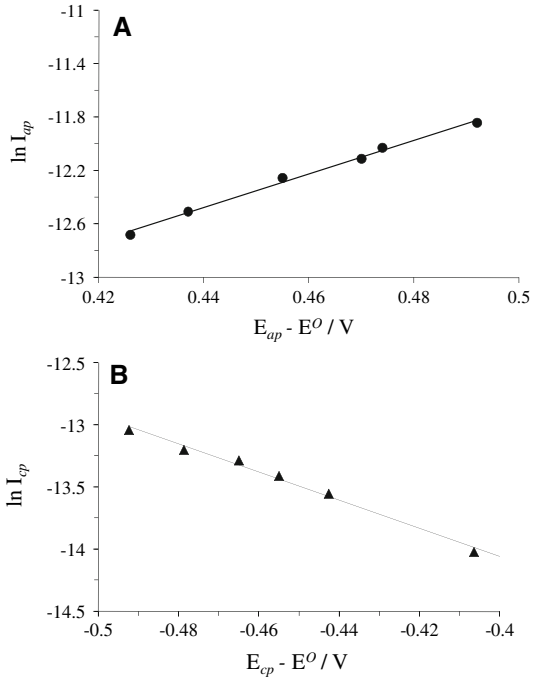

Fig. 5 Experimental variation of the peak current as a function of the difference $E_p - E^0$ (points) for both the anodic (*filled circle*) and cathodic (*filled triangle*) processes. The line results from the linear fitting of the experimental data **a** $\ln I_{pa} = 18.12$ (V^{-1}) $(E_{pa} - E^0) - 14.66$ and **b** $\ln I_{pc} = 18.97$ (V^{-1}) $(E_{pc} - E^0) - 15.6$

3.3 Cyclic voltammetry of the AA in the presence of CTAB

Figure 6 shows the CV's recorded from the system CPE/0.01 mM AA, x mM CTAB where $x \in \{0, 0.02, 0.04, 0.06, 0.09$ mM$\}$ at pH = 3. The CV from the AA without CTAB shows an oxidation peak at 503 mV: as the CTAB concentration increased the peak shifted toward smaller potentials (see Fig. 6B) thereby increasing its current intensity, although when the scan was reversed there were no reduction peaks displayed. Therefore, the process was an irreversible one. This behavior indicates that the oxidation process was favored due to the CTAB presence in the system. It is important to stress out that the previous methodology cannot be applied to determination of k^0 and the number electrons involved during the electrochemical reaction of AA since its CV is an irreversible one (it does not display a cathodic reduction peak), notwithstanding Wen et al., [25] have proposed that two electrons are involved during AA electrochemical oxidation.

From these results it is possible to note that the CTAB greatest influence was on the DA, because it disfavored its oxidation and reduction, thereby giving a smaller k^0, which is why the process tends to irreversibility. On the contrary, for the AA's case, its oxidation was favored; these effects can influence the separation of the DA's and the AA's voltammetric signals, which introduces the possibility to perform DPV studies.

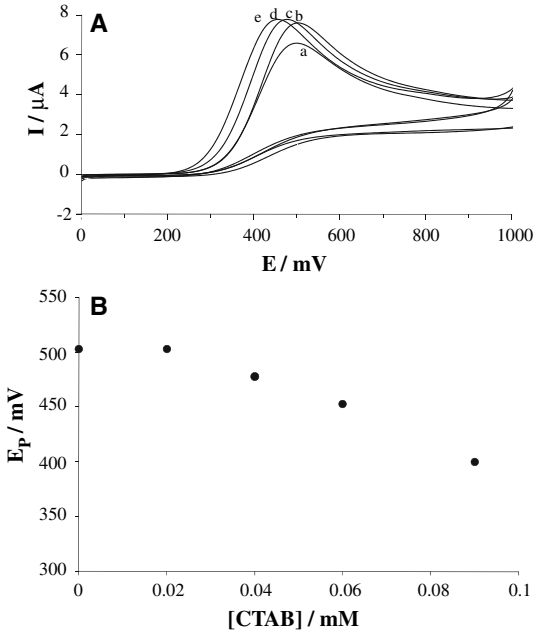

Fig. 6 **A** Family of experimental cyclic voltammograms recorded in the system CPE/AA 0.01 mM, *x* mM CTAB, where *x* is (a) 0, (b) 0.02, (c) 0.04, (d) 0.06, and (e) 0.09 mM at pH = 3. Scan rate 100 mV s^{-1} and **B** potential peak trend from the CV recorded under the conditions stated in (**A**) as a function of [CTAB]

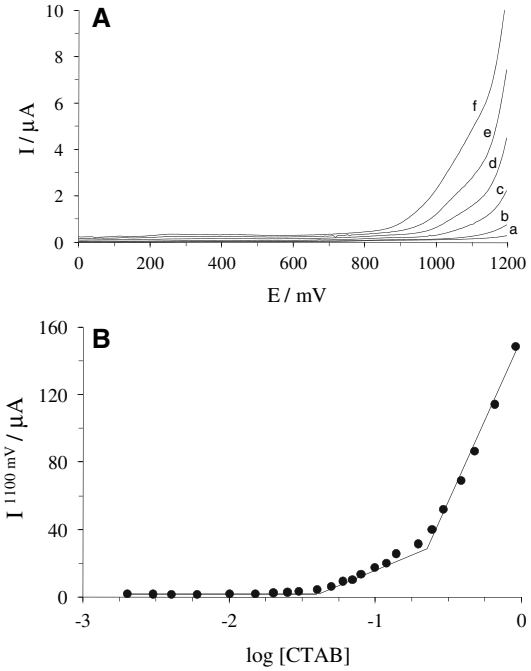

Fig. 7 **A** Family of experimental DPV recorded in the system CPE/*x* mM CTAB, where *x* is (a) 0, (b) 0.02, (c) 0.05, (d) 0.08, (e) 0.1, and (f) 0.3 mM at pH = 3. **B** Trend of I_p (1,100 mV) as a function of log [CTAB]. Scan rate 20 mV s^{-1}

3.4 Differential pulse voltammetry of the CTAB

Similarly to what was done during the CV, here the electrochemical behavior of the CTAB is analyzed by means of DPV. Figure 7 shows the DPV recorded in the system CPE/1 M NaCl, *x* mM CTAB where *x* ε {0.002, 0.02, 0.05, 0.08, 0.1, and 0.3 mM} at pH = 3. It is easy to note that as the CTAB concentration was increased in the system, there was an increase in the current intensity from approximately 800 mV. Plotting the current at a potential of 1,100, $I_p^{1,100\ mV}$ as a function of log [CTAB], produced the graph shown in Fig. 7B, where two slope changes can be noted; the first corresponds to a concentration of 0.042 mM, while the second corresponds to 0.27 mM.

Similarly to CV, there exists the CTAB interference problem for potentials above 800 mV, which leads to the necessity to perform studies for the DA and the AA to verify that there was no interference between the two analytes.

3.5 Differential pulse voltammetry for DA and AA

Figure 8A shows the DPV's recorded in the system CPE/0.01 mM DA, *x* mM CTAB, where *x* is (a) 0, (b) 0.008, (c) 0.02, (d) 0.08, (e) 0.12, (f) 0.16, and (g) 0.3 mM at pH = 3, DA without CTAB presents one oxidation peak at 634 mV, though when adding CTAB this peak's current decreases and shifts toward greater potential values, to locate itself finally at around 900 mV. This trend can be noted more clearly in Fig. 8B, where the effect is due to the electrostatic interaction between the CTAB and the DA and because the charge transfer is slower. However, as mentioned before, the CTAB signal interferes with that of the DA for concentrations above 0.3 mM, which can limit its quantification at greater concentrations of the surfactant.

DPVs were also recorded in the system CPE/0.01 mM AA, *x* mM CTAB, where *x* ε {0, 0.01, 0.04, 0.05, 0.06, 0.08, and 0.1 mM} at pH = 3 (not shown). The AA oxidation peak was located at 439 mV and shifted up to 350 mV as CTAB concentration was increased in the system, thus favoring AA oxidation.

3.6 Electrochemical study of the DA and the AA in the presence of CTAB

Using DPV to perform also the study on the DA in the presence of AA, gave the results shown in Fig. 9; they depict the behavior of the two analytes at different CTAB concentrations ranging from 0.002 to 0.1 M. Without CTAB, the DA's peak, P_{DA}, appears at 695 mV, while that of AA, P_{AA}, at 513 mV, which gives a peak separation of 182 mV, however, signal's overlap is still evident. When the CTAB was added to the system, the signal of the AA shifts toward smaller potentials, whereas the DA's peak shifted the opposite way, to greater potentials, giving thus a

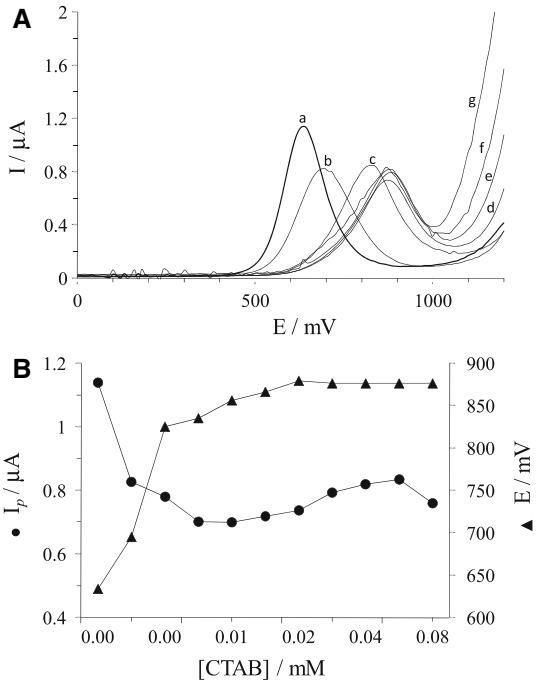

Fig. 8 **A** Family of experimental DPV recorded in the system CPE/0.01 mM DA, *x* mM CTAB, where *x* is (a) 0, (b) 0.008, (c) 0.02, (d) 0.08, (e) 0.12, (f) 0.16, and (g) 0.3 mM at pH = 3. Scan rate 20 mV s^{-1}. **B** Tendency of (*filled triangle*) E_p and (*filled circle*) I_p as a function of [CTAB]

peak separation up to 453 mV, which is larger than that reported by other authors [28, 32–45].

Table 2 shows the peak separation for the AA and DA as a function of [CTAB]. The increased separation is noted as a function of increasing [CTAB].

These studies show that the use of the surfactant induced the electrochemical separation between the DA and the AA, even in the light of the argument that the CTAB's signal may happen to interfere during the quantification. Therefore, the following experiments are carried out aiming to determine the best experimental conditions to design a method for the analytic quantification of the DA in the presence of AA.

3.7 Optimization of the experimental conditions

3.7.1 Effect of the pH

Considering the CTAB's electrostatic interactions with the analytes and taking into account that the AA's *p*Ka = 4.17 [46], a study was performed at pH = 6.23 so that the AA is negatively charged and that the DA is positive, seeking to improve the separation.

3.7.1.1 pH = 6.23 Figure 10A, shows the DPV's recorded in the system CPE/NaCl 0.1 M, CTAB 0.03 mM, AA

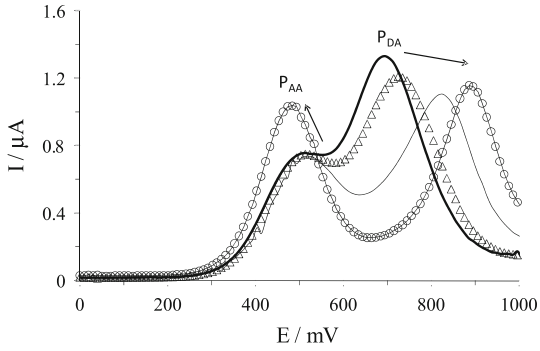

Fig. 9 Family of experimental DPVs recorded in the system CPE/0.01 mM AA, *x* mM CTAB, where *x* is (*thick line*) 0, (*open triangle*) 0.002, (*thin line*) 0.004, and (*open circle*) 0.04 mM. Scan rate 20 mV s^{-1}

Table 2 Variation of the voltammetric parameters as a function of [CTAB], corresponding to the CVs shown in Fig. 9

[CTAB] (mM)	E_P^{AA} (mV)	E_P^{DA} (mV)	$E_P^{AA} - E_P^{DA}$ (mV)	I_p^{AA} (µA)	I_p^{DA} (µA)
0	513	695	182	0.75	1.33
0.002	513	725	212	0.75	1.21
0.004	523	826	303	0.73	1.11
0.006	523	846	323	0.73	1.08
0.008	523	856	333	0.73	1.12
0.010	523	856	333	0.73	1.12
0.012	523	876	353	0.77	1.12
0.016	523	886	363	0.84	1.14
0.020	523	896	373	0.85	1.14
0.040	493	906	413	1.03	1.18
0.050	459	886	426	1.16	1.14
0.060	443	886	443	1.23	1.09
0.080	433	886	453	1.25	1.03

0.5 mM at pH = 6.23 and various DA concentrations. From Fig. 10A it becomes possible to appreciate that the AA's oxidation peak, P_{AA}, was recorded at 327 mV while that of the DA, P_{DA}, appeared at 805 mV; thus, the peak separation was 478 mV. Although as the DA concentration increases in the system, another oxidation peak begins to be recorded at 620 mV, particularly when [DA] > 0.08 mM, see Fig. 10A. This effect limits the DA's quantification in commercially available samples, as this peak may correspond to some species that was not considered in the analysis. When constructing the DA's calibration plot, that shown in Fig. 10B was obtained; the linear fit gave the following expression for a straight line: I_p^{DA} (µA) = 0.005[DA](µA $µM^{-1}$) + 0.09 (µA) and a correlation coefficient $r^2 = 0.995$. Calculating some of the analytic parameters using the data from the plot, a linearity range 0–168 µM, a sensitivity of 0.005 µA $µM^{-1}$, a detection limit, DL, of 11 µM and a quantification limit, QL, of 36 µM, were obtained.

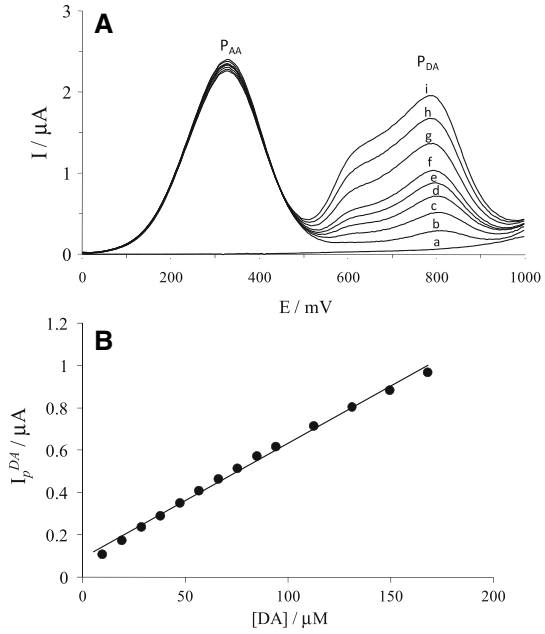

Fig. 10 **A** Family of experimental DPVs recorded in the system CPE/NaCl 0.1 M, CTAB 0.03 mM, AA 0.5 mM at pH = 6.23 with different [DA]: (a) 0, (b) 0.04, (c) 0.08, (d) 0.11, (e) 0.15, (f) 0.19, (g) 0.27, (h) 0.37, and (i) 0.45 mM, at 20 mV s^{-1} scan rate. **B** Calibration plot obtained from the DPV's, as those shown in (**A**), for [DA] < 0.27 mM, the *solid line* resulted from the linear fitting of the experimental results (*filled circle*)

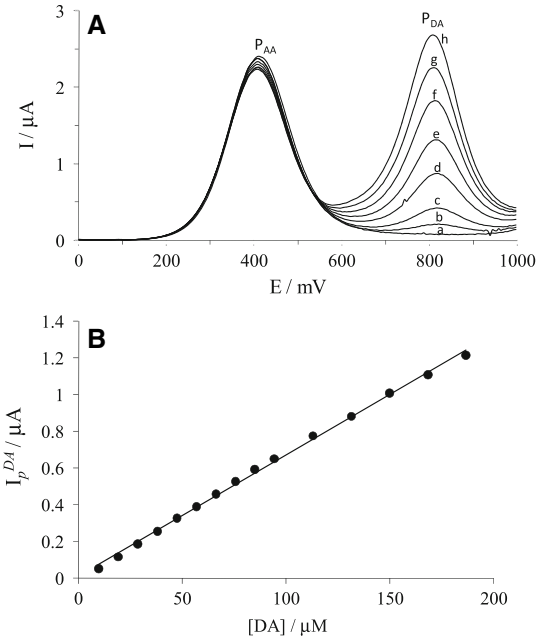

Fig. 11 **A** Family of experimental DPV recorded in the system CPE/NaCl 0.1 M, CTAB 0.03 mM, AA 0.5 mM at pH = 3 with different [DA]: (a) 0, (b) 0.02, (c) 0.05, (d) 0.11, (e) 0.17, (f) 0.23, (g) 0.37, and (h) 0.54 mM at 20 mV s^{-1} scan rate. **B** Calibration plot obtained from the DPV's, as those shown in (**A**), for [DA] < 0.23 mM, the *solid line* resulted from the linear fitting of the experimental results (*filled circle*)

3.7.1.2 pH = 3 Figure 11A, shows the DPVs recorded in the system CPE/NaCl 0.1 M, CTAB 0.03 mM, AA 0.5 mM at pH = 3 and various DA concentrations. From the plot it can be noted that the P_{AA} is located at 410 mV while the P_{DA} was recorded at 815 mV; the peak separation was 405 mV, which is slightly smaller than that obtained at pH = 6.23, in fact 73 mV. However, there were no recordings of additional peaks from either, the DA or the AA. The calibration plot that resulted is shown in Fig. 11B, and the following were the analytic parameters obtained: linearity range 0–186 µM, sensitivity 0.007 µA $µM^{-1}$, DL 11 µM, and QL 37 µM.

With these results it appears simple to underline the influence of the pH over the systems studied thus far. This leads to the preliminary conclusion: pH = 3 was the best to carry out the DA determinations, because there were only the oxidation peaks of the corresponding analytes, also giving the best set of analytic parameters. After determining the best pH with which to develop the work, the results concerning different CTAB concentrations will be presented next.

3.7.2 Effect of the CTAB concentration

Figure 12 shows some DPV's recorded in the systems CPE/NaCl 0.1 M, AA 0.5 mM at pH = 3 for various DA and CTAB concentrations. It can be noted that in Fig. 12A, the P_{AA} was recorded at 405 mV, though when the DA was added to the system, the P_{DA} then shifted to 825 mV. However, as the [DA] was increased in the system, the P_{AA} was displaced toward smaller potentials, bearing current fluctuations. Figure 12B shows that the P_{AA} was recorded at 410 mV whereas the P_{DA} was recorded at 815 mV, which when compared to Fig. 12A, the P_{AA} did not register any change as the [DA] changed in the system. Figure 12C displays a similar effect to that shown in Fig. 12A because the P_{AA} (a) was recorded at 405 mV, but when the [DA] was increased in the system, it shifted toward greater potentials and the current signal exhibited fluctuations. Aside this effect, it can be observed that for [DA] > 0.2 mM there was the presence of another oxidation peak at 610 mV. Lastly from Fig. 12D the P_{AA} (a) was at 371 mV and when the DA is present in the system, it shifted toward smaller potentials, like 346 mV, and remains constant. However, the Gaussian-shaped resulting peak, P_{DA}, located at 795 mV, may indicate the contribution of another species present in the system, because the peak similarity respect to those shown in Fig. 12A and B.

A calibration plot was produced for each of the plots shown in the previous Fig. 12 and the corresponding analytic parameters were calculated: they are presented in Table 3.

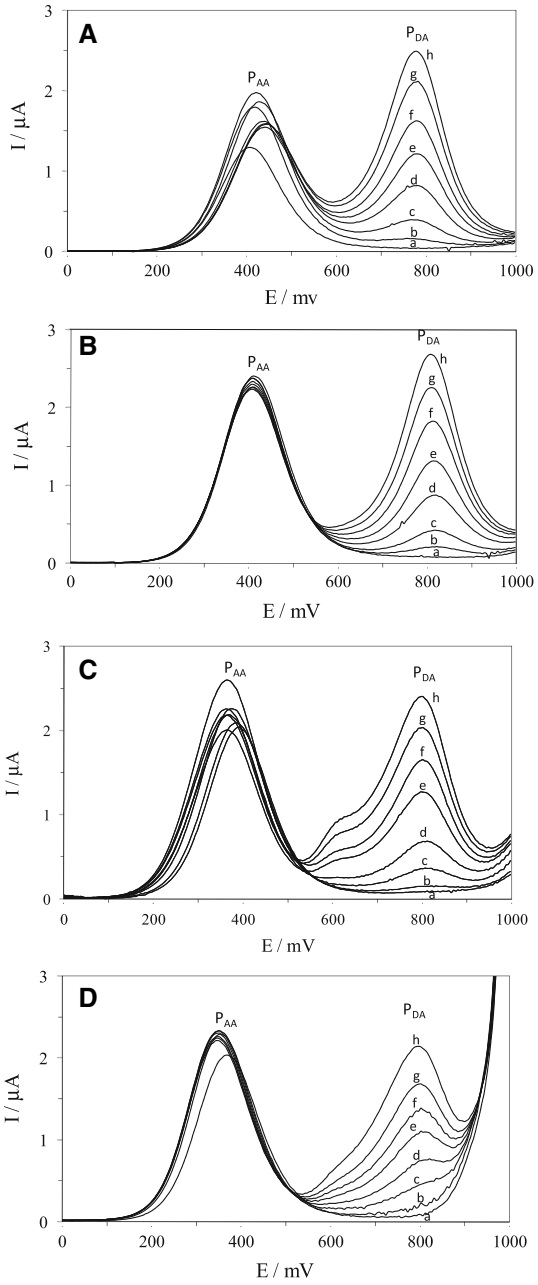

Fig. 12 Family of experimental DPVs recorded in the system CPE/NaCl 0.1 M, AA 0.5 mM at pH = 3 with different [DA]: (a) 0, (b) 0.01, (c) 0.05, (d) 0.11, (e) 0.19, (f) 0.28, (g) 0.37, and (h) 0.45 mM and at different [CTAB] **A** 0.01, **B** 0.03, **C** 0.5, and **D** 1.0 mM. The scan rate was 20 mV s^{-1} in all cases

From these results it can also be concluded in a preliminary manner, that the best [CTAB] was 0.03 mM, because before this concentration value, see Fig. 12A, the AA's oxidation seemed rather an unstable occurrence, with apparent signal fluctuations. When the [CTAB] > 0.03 mM, see Fig. 12B and C there were two peaks within the zone of the DA's oxidation peak, plus the analytic parameters shown in Table 3, leads one to note that the system displayed smaller detection and quantification limits and a greater concentration interval.

3.7.3 Effect of the AA concentration

Figure 13, shows the family of DPVs for the systems CPE/NaCl 0.1 M, CTAB 0.03 mM, with various DA and AA concentrations, namely, (A) 0.03, (B) 0.05, (C) 0.08, and (D) 0.10 mM, at pH = 3. It can be noted that, with the exception of Fig. 13B, the AA current signal fluctuates. The analysis of the DA signal, as observed in Fig. 13D, shows that it is lower though not as quantifiable as that shown in Fig. 13B, because even if its the same [DA], the signal is better in the latter trace.

Calibration plots were produced for each of the systems, see Fig. 13, and the analytic parameters calculated are shown in Table 4.

These results lead to stating that the [AA] influences the analytic response of the DA and that 0.05 mM was the best AA concentration to perform the analysis, because of the following: thereat the AA signal remained constant, a greater linearity interval was attained, even though the detection limit was smaller than 0.08 M in the system and the sensitivity was better.

3.7.4 Effect of the potential scan rate

Figure 14 shows two DPV families for the system CPE/NaCl 0.1 M, AA 0.05 mM, CTAB 0.03 mM, at pH = 3, at various DA concentrations and different scan rates, namely, (A) 20 mV s^{-1} and (B) 50 mV s^{-1}. From the figures it is clear that the scan rate also influences the DA and AA signals, particularly the latter, because at 50 mV s^{-1} three oxidation peaks were recorded, where the opposite is true for the trace in Fig. 14A that shows only

Table 3 Analytical parameters obtained from the DA calibration curves for the system: CPE/NaCl 0.1 M, AA 0.5 mM at pH = 3 as a function of [CTAB]

[CTAB] (mM)	Linear range (µM)	Sensitivity (µA mM^{-1})	Detection limit (µM)	Quantification limit (µM)
0.01	0–186	6.321±0.002	15±0.2	51±0.2
0.03	0–186	6.654±0.001	11±0.1	37±0.2
0.5	0–130	6.383±0.002	11±0.1	37±0.2
1	0–93	7.390±0.003	11±0.2	34±0.3

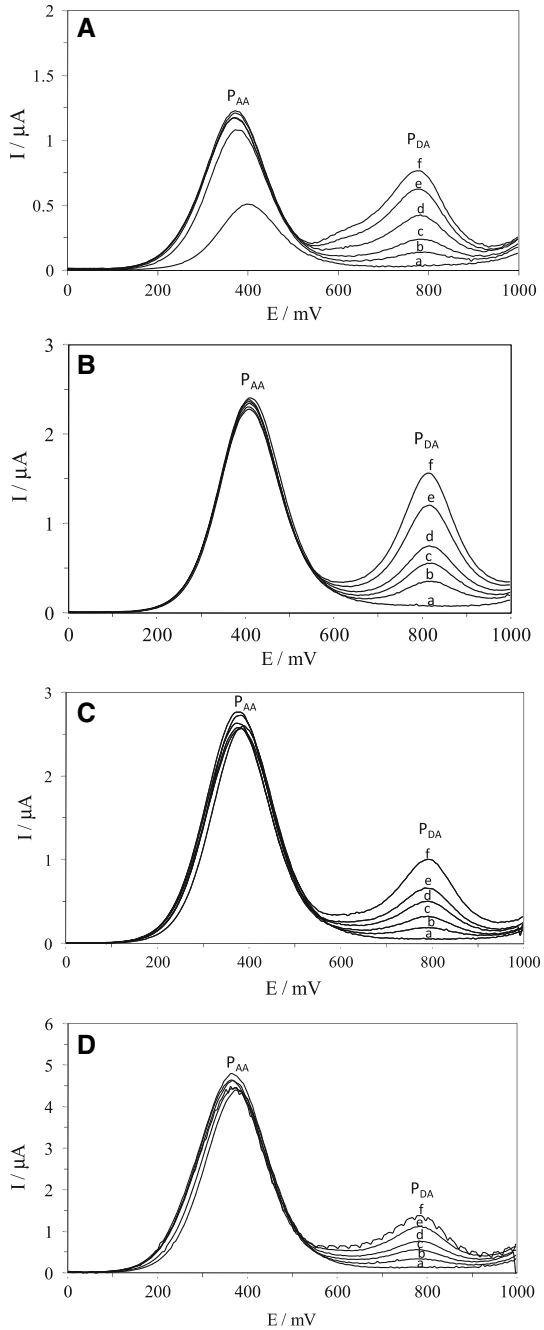

Fig. 13 Family of experimental DPV recorded in the system CPE/NaCl 0.1 M, CTAB 0.03 mM with different [DA]: (a) 0, (b) 0.04, (c) 0.06, (d) 0.10, (e) 0.15, and (f) 0.20 mM and different [AA] **A** 0.03, **B** 0.05, **C** 0.08, and **D** 0.10 mM at pH = 3. Scan rate 20 mV s^{-1}

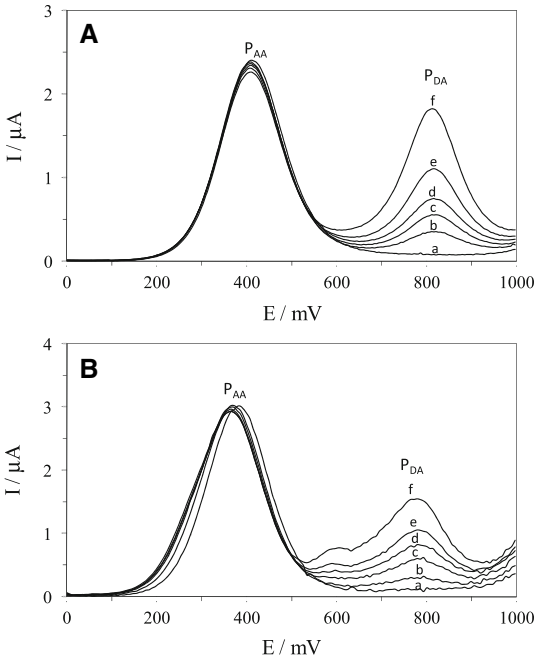

Fig. 14 Family of DPVs recorded in the system CPE/NaCl 0.1 M, AA 0.05 mM, CTAB 0.03 mM with different DA concentrations, namely: (a) 0, (b) 0.04, (c) 0.07, (d) 0.10, (e) 0.15, and (f) 0.23 mM, at pH = 3, with different scan rates: **A** 20 mV s^{-1} and **B** 50 mV s^{-1}

the AA and the DA peaks. Thus, the best rate to work at was 20 mV s^{-1}.

With these results it becomes possible to formulate the set of optimal analytic conditions, as follows: pH = 3, [CTAB] = 0.03 mM, [AA] = 0.5 mM, and 20 mV s^{-1} scan rate, which will be used to carry out the analytic determination using a real pharmaceutical sample.

3.8 Recovery analysis

The use of the optimized experimental conditions stated above permitted to obtain four calibration plots now used to formulate an expression to describe the uncertainty of the measurements: I (μA) = 0.0063 ± 0.0002 (μA μM^{-1}) [DA] + 0.0015 ± 0.0005 (μA); the resulting correlation coefficient was 0.9995. The analysis of the resulting parameters for this system gave: a linearity range of 0–130 μM, a detection limit of 11 μM and a sensitivity of 0.0063 ± 0.0002 μA μM^{-1}. After the calibration plots

Table 4 Analytical parameters obtained from the DA calibration plots for the system: CPE NaCl 0.1 M at pH = 3, CTAB 0.03 mM as a function of [AA]

[AA] (mM)	Linear range (μM)	Sensitivity (μA mM^{-1})	Detection limit (μM)	Quantification limit (μM)
0.03	29–114	4.595±0.002	14±0.1	46±0.1
0.05	0–130	6.318±0.002	11±0.1	37±0.2
0.08	0–91	5.978±0.002	10±0.1	37±0.1
0.1	0–98	7.845±0.003	11±0.2	38±0.1

Table 5 Recovery for the system CPE/NaCl 0.1 M, CTAB 0.03 mM, AA 0.5 mM at pH = 3

Measurement	Expected value (mM)	Calculated value (mM)	Recovery (%)
1	0.0754	0.0747	99.10
2		0.0749	99.28
3		0.0736	97.99
	Standard deviation	0.0007	

Table 6 Results of the DA determination from a commercially available pharmaceutical injectable solution

DA content (mg mL^{-1})	DA found (mg mL^{-1})	% Error
40	38	5

were produced, another analytic parameter was obtained, called the recovery. In order to evaluate this, three measurements were undertaken as shown in Table 5.

The data presented in Table 5 suggest satisfactory results for the systems studied, since the recovery was 98.79 ± 0.70%. Next, the results of the analysis performed on the commercially available pharmaceutical, an injectable solution from Kendrick, 200 mg/5 mL.

3.9 Analysis of the pharmaceutical

A 100 μL aliquot is taken from the injectable solution and is brought to 10 mL using NaCl 0.1 M at pH = 3; from this 300 μL were taken into a cell containing 10 mL of the system NaCl 0.1 M, [CTAB] 0.03 mM, and [AA] 0.5 mM. A DPV is taken from the resulting cell solution and the DA concentration was evaluated through the expression I (μA) = 0.0063 ± 0.0002 (μA μM^{-1}) [DA] + 0.0015 ± 0.0005 (μA) that resulted from the calibration plot. Three measurements were performed on the pharmaceutical; and the results obtained are presented in Table 6.

The results above lead to conclude that the CTAB and the CPE allow separation of the DA and the AA signals, at the same time that the DA's analytic determination was carried out from an injectable solution, giving good results, because the linearity range was sufficiently ample and a detection limit was of the μM order, displaying a good sensitivity that can be compared with results from the literature. However, the greatest advantage is that the CPE electrode used is plainly affordable because of its low cost.

4 Conclusions

This work shows that CTAB influences the DA behavior as its oxidation mechanism becomes more irreversible, thus disfavoring either oxidation or reduction, consequently provoking that the heterogeneous rate constant, k^0, decreases drastically. This effect helps to bring in the electrochemical separation of the DA and AA peaks up to 453 mV. Optimization of the experimental methods, permitted to identify the best set of [CTAB] and [AA] concentrations, the best solution pH and potential scan rate, to derive from them all the analytic parameters, such as: 0–130 μM linearity range, 0.0063 ± 0.0002 μA μM^{-1} sensitivity, 11 μM detection limit, and 37 μM quantification limit, with which to apply the method for the analytic determination on a commercial injectable pharmaceutical, obtaining satisfactory results.

Acknowledgments The authors would like to thank the Red ALFA II for the BioSenIntg Clave: II-0486-FCFA-FCD-FI Project. Also, SCA 58250 and GAA 105024 express their gratitude to CONACyT for their postdoctoral grants. MTRS thanks CONACyT for support through Project 82932 and SCA for Project 80305. Also SCA, MARR, MEPP, and MTRS gratefully thank the SNI for the distinction of their membership and the stipend received. SCA, MEPP, and MARR wish to thank the Departamento de Materiales, UAM-A, for the financial support given through Projects 2260220, 2260231, and 2260234.

References

1. El Kommos ME, Mohamed FA, Khedr ASK (1990) J Assoc Anal Chem 73:516
2. Sorouraddin MH, Manzoori JL, Kargarzadeh E, Ají Shabani AM (1998) J Pharm Biomed Anal 18:877
3. Stetter JR, Penrose WR, Yao S (2003) J Electrochem Soc 150: S11
4. Venton BJ, Wightman RM (2003) Anal Chem 1:414A
5. Chen J, Cha CS (1999) J Electroanal Chem 463:93
6. Dayton MA, Ewing AG, Wightman RM (1980) Anal Chem 52:2392
7. Zhang Y, Cai Y, Su S (2006) Anal Biochem 350:285
8. Yogeswaran U, Thiagarajan S, Chen SM (2007) Anal Biochem 365:122
9. Yin T, Wei W, Zeng J (2006) Anal Bioanal Chem 386:2087
10. Li J, Lin XQ (2007) Anal Chim Acta 596:222
11. Yao H, Sun Y, Lin X, Tang Y, Liu A, Li G, Li W, Zhang S (2007) Anal Sci 23:667
12. Jiang XH, Lin XQ (2005) Anal Chim Acta 537:145
13. Chen SM, Peng KT (2003) J Electroanal Chem 547:179
14. Gong JM, Lin XQ (2004) Electrochim Acta 49:4351
15. Sánchez-Rivera AE, Vital-Vaquier V, Romero-Romo M, Ramírez-Silva MT, Palomar-Pardavé M (2004) J Electrochem Soc 151:C666
16. Rusling JF (1991) Acc Chem Res 24:75
17. Kaifer AE, Bard AJ (1985) J Phys Chem 89:4876
18. Ouiatela DA, Diaz A, Kaifer AE (1988) Langmuir 4:663
19. Davidovic A, Tabakovic I, Davidovic D, Duic L (1990) J Electroanal Chem 280:371
20. Wen XL, Han ZX, Rieker A, Liu ZL (1997) J Chem Res (S) 3:108.
21. Wen XL, Han ZX, Rieker A, Liu ZL (1998) J Chem Soc Perkin Trans 2:905
22. Connors TF, Rusling JF, Owlia A (1985) Anal Chem 57:170
23. Stadlober M, Kalcher K, Raber G, Neuhold C (1996) Talanta 43:1915

24. Chen SM, Chzo WY (2006) J Electroanal Chem 587:226
25. Wen XLW, Jia YH, Liu ZL (1999) Talanta 50:1027
26. dos Reis AP, Tarley CRT, Maniasso N, Kubota LT (2005) Talanta 67:829
27. Corona-Avendaño S, Alarcón-Angeles G, Ramírez-Silva MT, Rosquete-Pina G, Romero-Romo M, Palomar-Pardavé M (2007) J Electroanal Chem 609:17
28. Alarcón-Angeles G, Corona-Avendaño S, Ramírez-Silva MT, Rojas-Hernández A, Romero-Romo M, Palomar-Pardavé M (2008) Electrochim Acta 53:3013
29. Ramírez MT, Palomar ME, González I, Rojas-Hernández A (1995) Electroanal 7:184
30. Martínez R, Ramírez MT, González I (1998) Electroanalysis 10:336
31. Yu L, Lu T, Yu-Xia L, Liu J, Gui-Ying X (2005) Colloid Surf A 257:375
32. Chen M, Li H (1998) Electroanalysis 10:477
33. Zhang Y, Jin G, Wang Y, Yang Z (2003) Sensors 3:443
34. Raj CR, Ohsaka T (2004) J Electroanal Chem 496:44
35. Ciszewski A, Milczarek G (1999) Anal Chem 71:1055
36. Raoof JB, Ojani R, Nadimi SR (2005) Electrochim Acta 50:4694
37. Jin GP, Lin XQ, Gong JM (2004) J Electroanal Chem 569:135
38. Zhang L, Sun YG (2001) Anal Sci 17:939
39. Lin XQ, Zhang L (2001) Anal Lett 34:1585
40. Zare HR, Rajabzadeh N, Nasirizadeh N, Ardakani MM (2006) J Electroanal Chem 589:60
41. Shankaran DR, Lmura K, Kato T (2003) Sensor Actuat B 94:73
42. Fang B, Zhang W, Kana X, Tao H, Denga X, Li M (2006) Sensor Actuat B 117:230
43. Lin X, Zhang Y, Chen W, Wu P (2007) Sensor Actuat B 122:309
44. Lin X, Zhuang Q, Chen J, Zhang S, Zheng Y (2007) Sensor Actuat B 125:240
45. Deakin MR, Kovach PM, Stutts KJ, Wightman RM (1966) Anal Chem 58:1474
46. Wang Q, Li N, Wang W (2002) Anal Sci 18:635